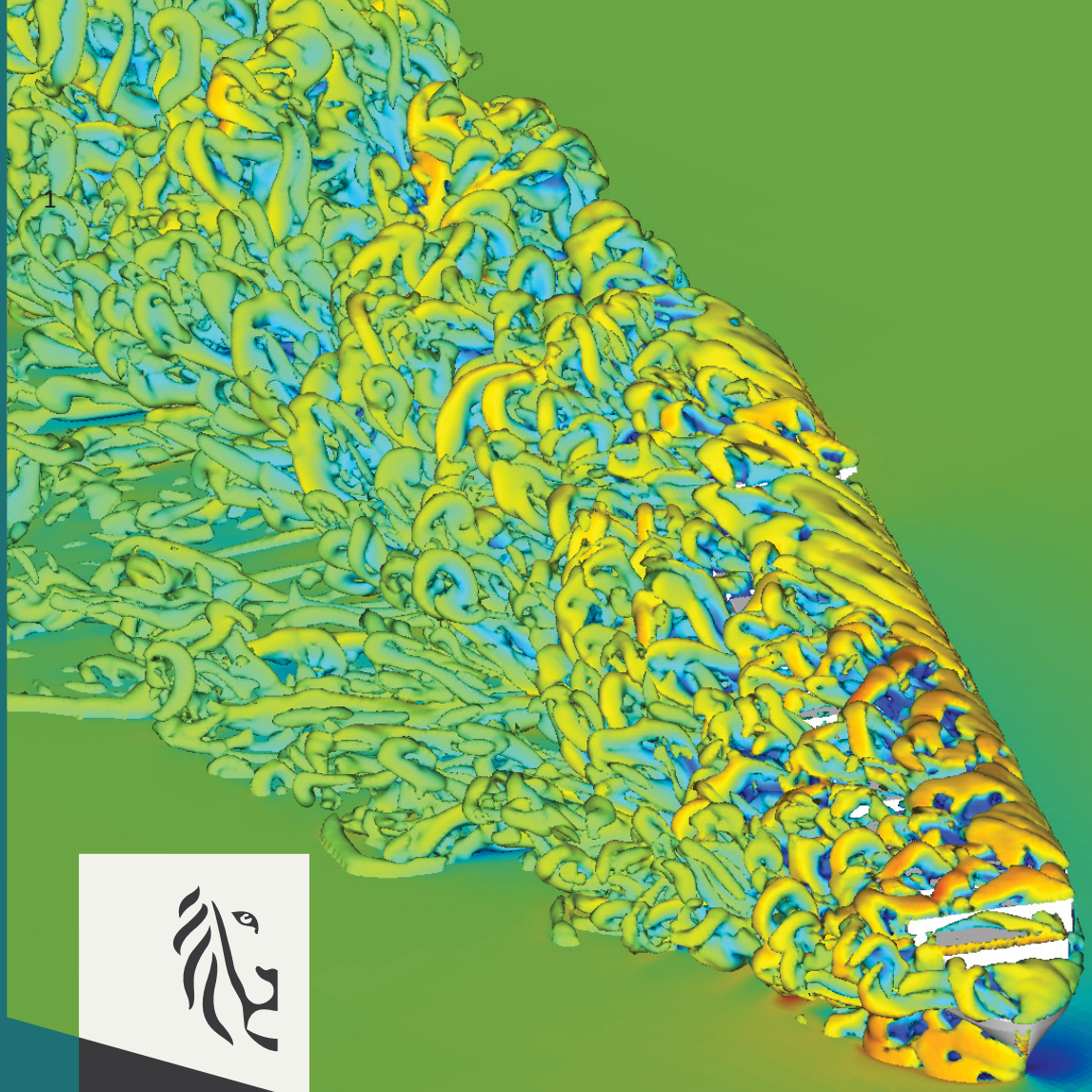

Flanders
State of
the Art

17_025_2
FH Reports

Computation of Rudder Open Water Characteristics

Grand Princess (F01) and Al Shamal (G01)

DEPARTMENT
MOBILITY &
PUBLIC
WORKS

www.flandershydraulics.be

Computation of Rudder Open Water Characteristics

Grand Princess (F01) and Al Shamal (G01)

Panahi, S.; Eloot, K.; Van Hoydonck, W.

Flanders Hydraulics
Flanders State of the Art

Cover figure © The Government of Flanders, Department of Mobility and Public Works, Flanders Hydraulics

Legal notice

Copyright and citation

D/2025/3241/021

This publication should be cited as follows:

Panahi, S.; Eloot, K.; Van Hoydonck, W. (2025). Computation of Rudder Open Water Characteristics: Grand Princess (F01) and Al Shamal (G01). Version 4.0. FH Reports, 17_025_2. Flanders Hydraulics: Antwerp

Document identification

Customer:	Flanders Hydraulics	Ref.:	WL2025R17_025_2
Keywords (3-5):	Open water rudder characteristics, CFD, F01, G01		
Knowledge domains:	Harbours and waterways > Manoeuvring Behaviour > Open water > Numerical calculations		
Text (p.):	17	Appendices (p.):	9
Confidential:	No	☒ Available online	

Author(s):	Panahi, S.

Control

	Name	Signature
Revisor(s):	Eloot, K.	Getekend door:Eloot Katrien Eliane Getekend op:2025-05-28 16:05:53 +02:0 Reden:Ik keur dit document goed Eloot Katrien Vlaamse overheid
Project leader:	Van Hoydonck, W.	Getekend door:Wim Van Hoydonck (Sign Getekend op:2025-05-28 16:21:20 +02:0 Reden:Ik keur dit document goed Van Hoydonck Wim Vlaamse overheid

Approval

Head of division:	Bellafkih, A.	Getekend door:Abdelkarim Bellafkih (Sig Getekend op:2025-05-31 11:08:24 +02:0 Reden:Ik keur dit document goed Bellafkih Abdelkarim Vlaamse overheid

Abstract

This is the second report in 17_025 study that deals with the computation of rudder open water characteristics using FINE/Marine Computational Fluid Dynamics (CFD) software package. It examines the rudder open-water characteristics for two vessels, the Grand Princess and Al Shamal. These rudders are identified as F01 and G01 in the Flanders Hydraulics (FH) towing tank database, and are semi-balanced horn rudders. The CFD approach used here follows the setup from the previous reports on this project (Van Hoydonck *et al.*, 2024), adjusting the domains and mesh configurations particularly for this study. However, grid convergence study was already performed in the past; so, to avoid repeating the same processing, we have utilised the knowledge gained from previous rudder open-water simulations conducted at FH. Due to the inherently fluctuating nature of the computed force and moment coefficients in rudder open-water simulations, a Savitzky-Golay filter is applied to improve the smoothness of final results.

For each of the rudders, two geometries are generated for which CFD computations are executed to determine the influence of geometry modifications: sharp edges chamfered, rudder and horn (combined in a spade rudder geometry). The first geometry is referred to as the ”base” configuration (with separate horn and blade), and the second is addressed as the ”simplified” configuration (spade rudder). The results are presented in terms of longitudinal force, lateral force and yawing moment coefficients, and a comparison is made between the current numerical findings and the existing experimental data.

The CFD results exhibit qualitatively correct trends over the investigated range of angles of attack. However, significant discrepancies are observed between the numerical and experimental data, especially for the lift coefficient. The main reasons for this are the disparity in Reynolds number between the towing tank tests and the numerical results, and the lack of inclusion of the horn in the experiments to determine the open water characteristics on the blade.

Contents

List of Figures

List of Tables

Nomenclature

Abbreviations

CAD	Computer Aided Design
CFD	Computational Fluid Dynamics
EFD	Experimental Fluid Dynamics
FH	Flanders Hydraulics

Latin symbols

b	Rudder height	m
c	Rudder chord length	m
L_{ref}	Reference length	m
N	Yawing moment coefficient	—
Re	Reynolds number	—
V_{ref}	Reference velocity	m/s
X	longitudinal force coefficient	—
Y	lateral force coefficient	—

Greek symbols

α	Angle of attack	rad
μ	Dynamic viscosity	Pas
ρ	Fluid density	kg/m^3
ω	Angular velocity	rad/s

1 Introduction

To develop mathematical models of vessels for use in the ship simulators at FH, towing tank tests are executed to assess the behaviour of vessels. Part of this process involved tests to determine the forces and moments acting on the rudder in open water, where the influence of the ship hull is absent (Vantorre, 2001). This data, along with open-water propeller characteristics, can be used to create mathematical manoeuvring models for the simulators at FH.

Recent investigation (Van Hoydonck *et al.*, 2018, 2017) shows that the Reynolds number at which open-water rudder characteristics are measured in the towing tank is much lower than at full scale. This discrepancy significantly impacts the accuracy of results, as the flow dynamics at model scale differ from those at full scale. At full scale, with attached flow conditions, the boundary layer is turbulent and stays attached along the rudder's entire chord, whereas at model scale, the flow is primarily laminar and detaches near the rudder's maximum thickness, which lead to differences in lift generation. Another issue to note is that the rudder section connected to the hull (known as the horn) is excluded from open-water tests, which has been found to notably affect both drag and lift coefficients.

To clarify further, in order to increase the Reynolds number during towing tank tests, both the scale factor and speed need to be increased. However, the current towing tank's limitations allow for a maximum Reynolds number of around 125,000 which is insufficient to trigger the natural transition of the boundary layer from laminar to turbulent flow. This transition can be forced by adding roughness elements near the rudder's leading edge, that may yield qualitatively accurate results. The fact that the horn was not included in the open water tests is influential as well. In realistic scenarios, the horn not only provides structural support but also influences the flow field and pressure distribution around the rudder, which impacts lift, drag, and rudder effectiveness.

Due to the focus of this project, the open-water characteristics of the F01 and G01 rudders determined based on models tests are presented in Fig. 1. As shown, both rudders indicate greater effectiveness in reverse flow conditions compared to normal flow conditions. The lift curve slope near α = 180° (reverse flow) is steeper than that observed near α = 0° (normal flow). $C_{L,max}$ in reverse flow is higher than or equal to that in normal flow, whereas it is generally expected to be higher under normal flow conditions. The drag coefficient at α = 0° is greater than at α = 180°, which is contrary to typical aerodynamic behaviour.

Considering the practical challenges that exist in the open-water rudder tests, in this report we conduct numerical simulations to determine open-water rudder characteristics of two semi-balanced horn rudders (F01 and G01), in which:

- The simulations are performed at full-scale conditions, allowing for a more accurate reproduction of the flow physics by simulating at representative Reynolds number.
- The presence of the rudder horn is included in the simulations, that enables the CFD analysis to account for the interaction between rudder and horn.
- Two different geometry configurations (simplified and base) are simulated, providing a basis for comparative analysis. This comparison can offer insights into how the existence of the gap between rudder and horn impacts the overall performance of the rudder, and the convergence characteristics of the computations when sharp edges are rounded.

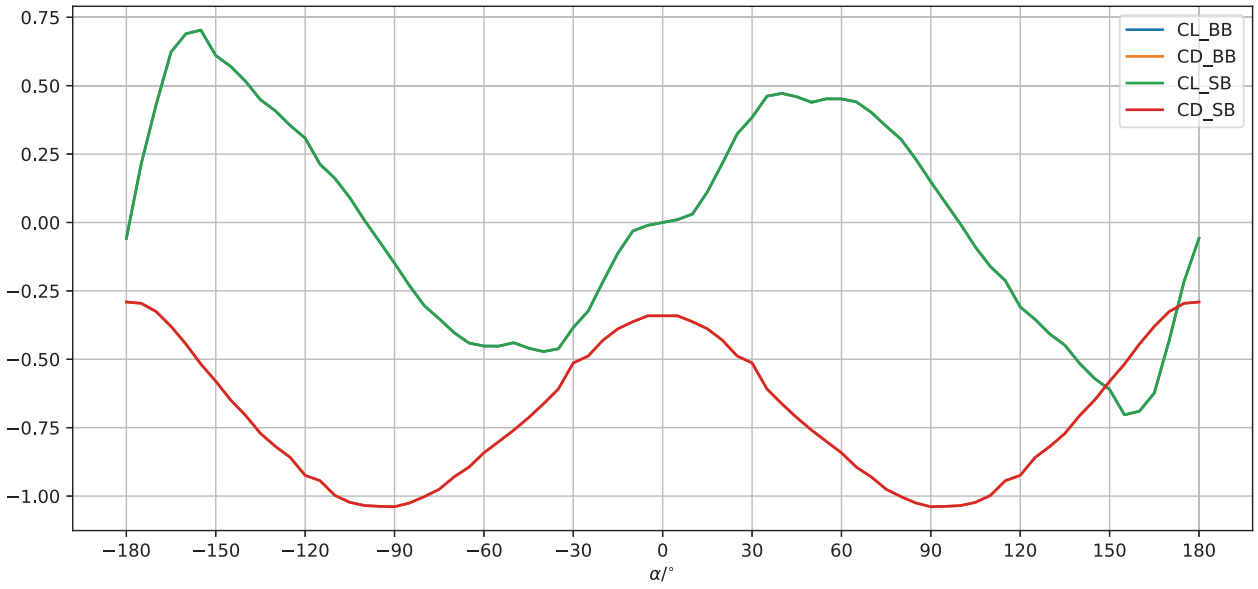

(a)

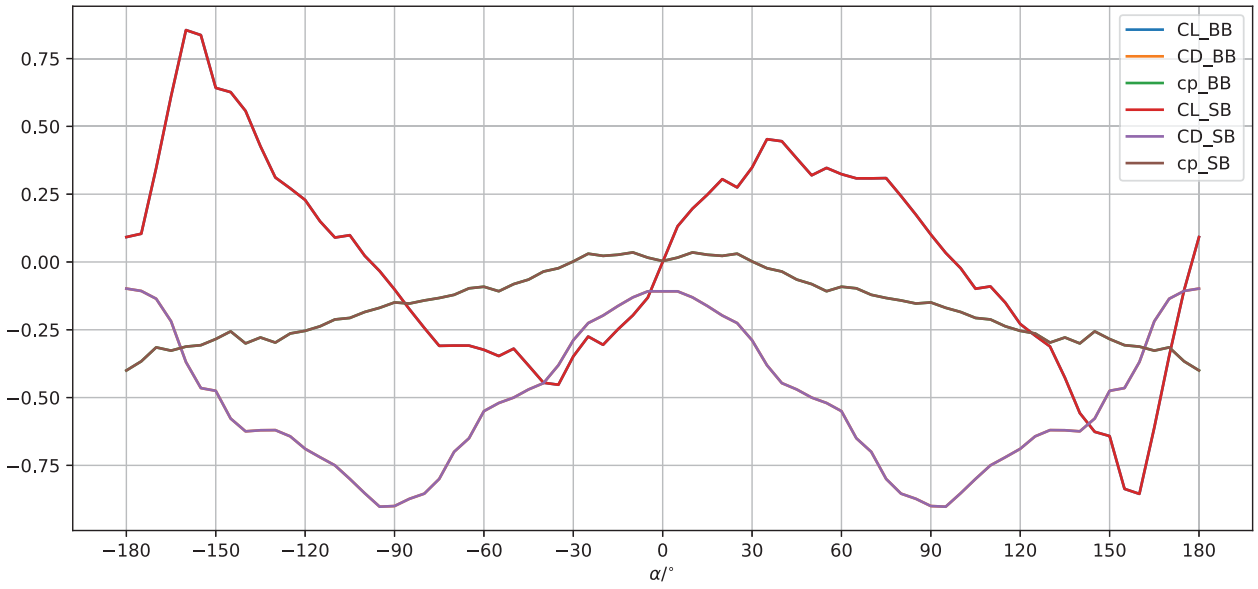

(b)

Figure 1 – Open water characteristics of (a) F01 rudder and (b) G01 rudder from model tests.

2 CFD analysis framework

2.1 Case study definition

This study investigates two rudders, F01 and G01. To facilitate comparison and achieve a more detailed analysis, each rudder has two defined geometries: simplified and base. This results in a total of four open-water CFD simulations conducted for the analysis. The simplified geometry consists of a single solid surface without any gap, while the base geometry includes the horn and rudder as separate geometries. Computer Aided Design (CAD) geometries of the considered rudders are illustrated in Fig. 2.

The flow is modelled as standard ITTC freshwater at a temperature of $15\,°$C, with a density of $\rho = 999.1026\,\mathrm{kg/m^3}$ and a dynamic viscosity of $\mu = 0.001\,138\,\mathrm{Pa \cdot s}$. Simulations are performed at full scale in unsteady mode, using a reference speed of $V_{ref} = 5\,\mathrm{m/s}$. The rudder rotates in the flow at an angular velocity of $\omega = 1\,°/\mathrm{s}$ for all computational cases. The characteristics of both rudder geometries are listed in Table 1. The Reynolds numbers for the F01 and G01 rudders, determined using their average chord lengths and the specified reference speed, are $Re = \frac{\rho V_{ref} c}{\mu} = 18.437 \times 10^6$ and 27.216×10^6 , respectively. The kinematic viscosity used in this case is $\nu = 1.1 \times 10^{-6}\,\mathrm{m^2/s}$.

Table 1 – Geometric characteristics of the full-scale rudders.

Rudder	Chord	Height	Thickness	Area	Aspect ratio
F01	$4.2\,\mathrm{m}$	$7\,\mathrm{m}$	$18\,\%$	$29.4\,\mathrm{m^2}$	1.66
G01	$6.2\,\mathrm{m}$	$10.4\,\mathrm{m}$	$19\,\%$	$64.48\,\mathrm{m^2}$	1.67

Drag, lift, and yaw moment coefficient curves are obtained from a single computation for each rudder separately. Typically, in this type of CFD computation, determining these coefficients involves averaging data from two distinct simulations: one with the rudder's angle of attack increasing and the other with it decreasing. However, since the rudder foil is symmetric, a single simulation covering an angle of attack range from $0°$ to $360°$ is sufficient to capture data for both cases. On the other hand, for an asymmetric rudder, two simulations would be required - one for counterclockwise rotation and another for clockwise rotation of the rudder in the domain - because the flow dynamics could differ, leading to different near-stall regions and hysteresis.

2.2 Computational domain

The rudder is placed within a cylindrical domain, with its top surface aligned to the cylinder's upper boundary (as shown in Fig.3). The exact dimensions of the computational domain for F01 and G01 are provided in Fig.4. As shown, the height and radius of the domain are adopted for the F01 and G01 rudders to accommodate for the different overall dimensions of the rudders (as detailed in Table 1). In general, the choice of such domains follows the best practices by the authors and is based on experience gained from previous computations. The centre of the rudder stock corresponds to the origin of the global axes system of FINE/Marine. As a result, the longitudinal force X is negative, which means $D = -X$. The lateral force (L) is positive to port side. The yawing moment is defined around the Z-axis and is positive when it tends to increase the angle of attack α of the rudder.

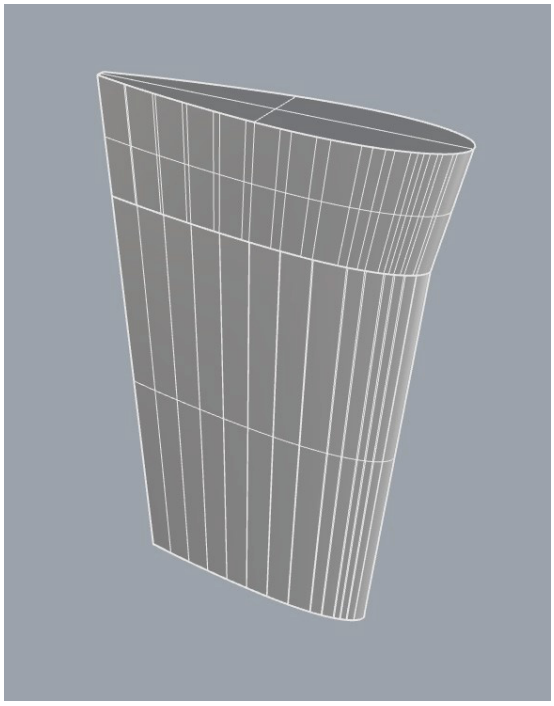

(a) CAD geometry of simplified F01.

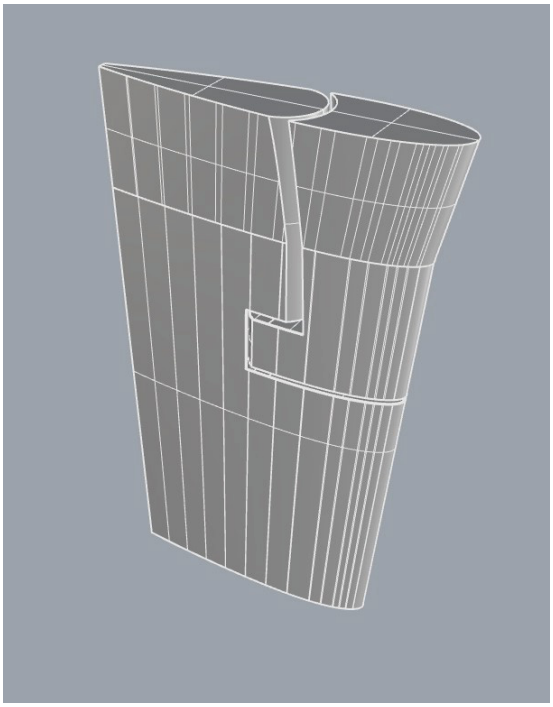

(b) CAD geometry of base F01.

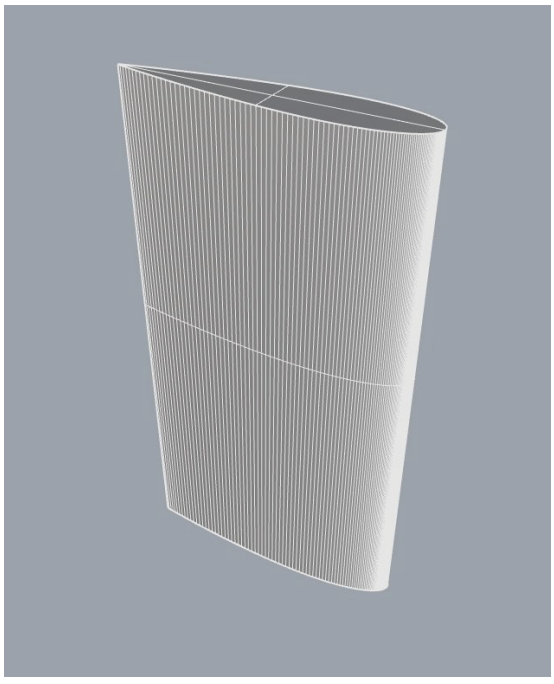

(c) CAD geometry of simplified G01.

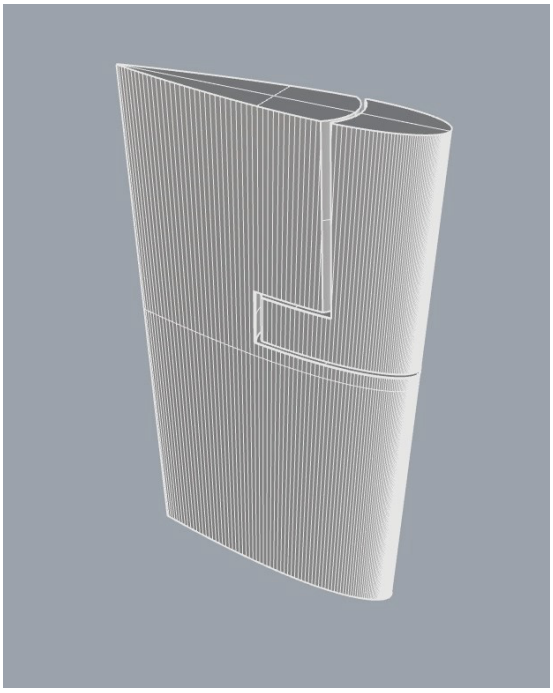

(d) CAD geometry of base G01.

Figure 2 – Perspective view of rudder CAD models.

2.3 Grid generation

2.3.1 Mesh setup

Hexpress starts its mesh generation process with an initial Cartesian mesh which encompasses the whole computational domain. The initial mesh corresponds to an isotropic subdivision of the computational domain

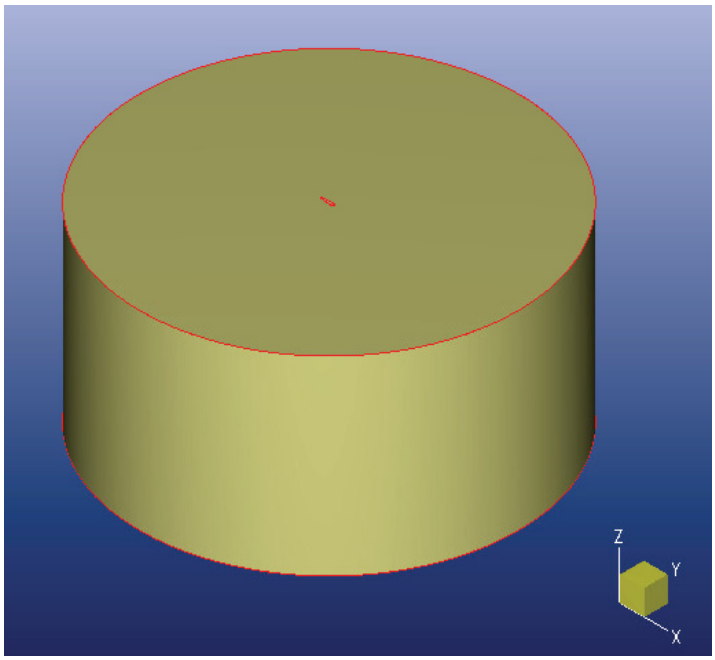

Figure 3 – Overall view of the computational domain.

bounding box. For all 4 computations of this study, the initial Cartesian mesh has $30 \times 30 \times 15$ cells. This leads us to have 13,500 number of cells at the first step of mesh generation.

As a conservative approach, the maximum number of global refinements is set to be 12. The cell sizes as function of refinement level for both geometries are shown in Table 2. Sufficient number of cells for the geometrical shape of the rudder can be considered, including areas near the leading edge (with the sharpest curvature) and the trailing edge (with the smallest geometric features: widths of $0.115\,\mathrm{m}$ for the F01 and $0.025\,\mathrm{m}$ for the G01 rudder). In order to ensure a smooth transition between fine and course cell regions, a refinement diffusion factor of 2 is applied. This means that the neighbours of a cell are flagged for refinement together with the neighbours of the neighbours. In this way, Hexpress creates square shaped refinement regions for the sake of grid smoothness.

Table 2 – Cell sizes as a function of subdivision level for both rudders.

Refinement level	Cell size (F01 rudder)	Cell size (G01 rudder)
0	5.3	6.3
1	2.65	3.15
2	1.325	1.575
3	0.6625	0.7875
4	0.331 25	0.393 75
5	0.165 625	0.196 875
6	0.082 812 5	0.098 437 5
7	0.041 406 25	0.049 218 75
8	0.020 703 125	0.024 609 375
9	0.010 351 562 5	0.012 304 687 5
10	0.005 175 781 25	0.006 152 343 75

In this project, the grid is constructed using a combination of curve refinements, surface refinements and box/volume refinements. The rudder's bottom curves are refined eight times, while the top curves are refined nine times to achieve optimal performance. For all cases, the design adheres to a maximum aspect ratio of

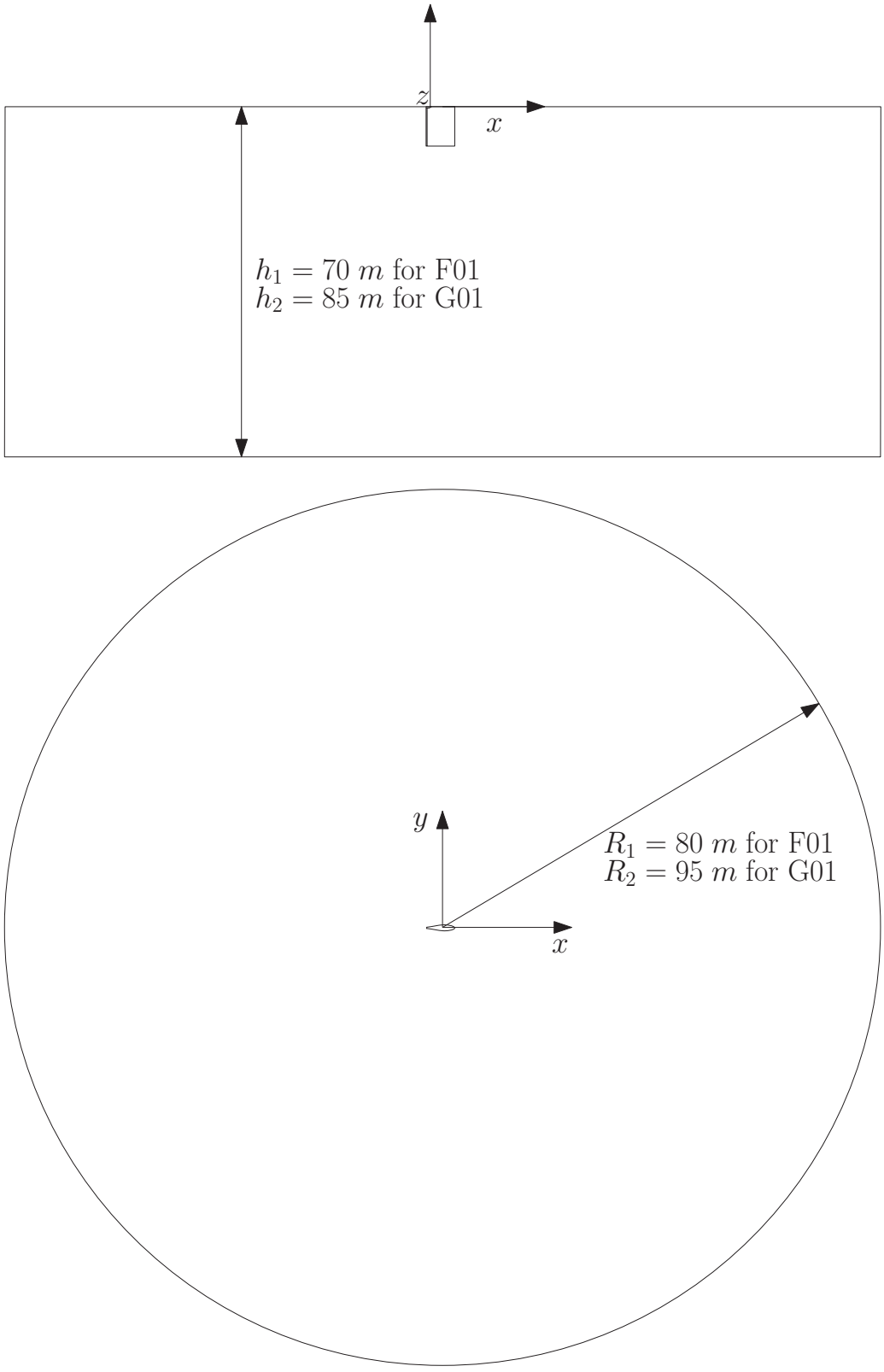

Figure 4 – Side view and top view of the domain.

2, with a curvature refinement factor set as 3.5. These parameters align with the best practices outlined by Hexpress User Guide. The top surface of the domain is refined twice; the rudder's trailing edge is refined nine times and its bottom surface seven times, all using the same configuration parameters. On the other hand, the side surface of the rudder undergoes 12 refinements, with target cell sizes of (0.063, 0.063, 0.063) and a curvature refinement factor of 60. This approach is employed to reduce cell sizes near the rudder's leading edge with the sharp curvature. During the simulations, it was observed that the default settings of Hexpress were not optimal for this scenario, as they failed to capture the flow precisely.

A cylindrical sector is added to refine the computational grid around the rudder. The refinement box has the features/details outlined in Table 3 for each rudder. In Table 3, the relative height is the ratio of the box height to the rudder height, and the relative maximum radius is the ratio of the box's maximum radius to the average chord length.

Table 3 – Refinement box details.

Rudder	Refinement box			
	Height		Maximum radius	
	Absolute value	Relative Value	Absolute value	Relative Value
F01	8 m	1.1428	5.5 m	1.3095
G01	11 m	1.0577	7 m	1.1290

Within these cylindrical volumes, the cells are refined five times. Trimming is also needed as the final step of this phase of grid generation. This step removes all the cells intersecting or located outside of the geometry. At the end, a staircase mesh will be produced including all the interior cells.

2.3.2 Snap to geometry and optimisation

All edges are captured in the snapping phase of the mesh generation. For buffer insertion, the top and bottom circular edges of the domain have type II while the edges of the rudder itself have type I. During the optimisation step, all settings were kept at their default values except minimal orthogonality threshold - which is increased to 15 degrees. A maximum of 5 orthogonality optimisation iterations are executed for cells with orthogonality less than 15 degrees.

2.3.3 Viscous layers

The final step in mesh generation involves setting the parameters for the viscous layer insertion. The specific details of the parameters along with the estimated first layer thickness by Hexpress (based on the knowledge gained from previous rudder open-water CFD simulations) are outlined in Table 4. It is important to note that a reference velocity of $5\,\mathrm{m/s}$ is maintained consistently across all simulations.

Table 4 – Viscous layer parameters.

Simulation no.	Investigated rudder	Reference length	Computed first layer thickness
1	Simplified F01	4.2 m	5.905×10^{-4} m
2	Base F01	4.2 m	5.905×10^{-4} m
3	Simplified G01	6.2 m	6.199×10^{-4} m
4	Base G01	6.2 m	6.199×10^{-4} m

For further clarification, the stretching ratio (the thickness ratio of the layers in the direction normal to the wall) is equal to 1.2. Floating number of viscous layers, ranging from 5 to 50, is considered when choosing

the inflation method. This approach allows Hexpress module to freely select the number of layers within the aforementioned predefined range.

After insertion of the viscous layers, the final number of cells for each computation as well as the respective minimum orthogonality are prescribed in Table 5. As observed, despite efforts to keep consistency in the meshes generated for rudders with and without gaps, the number of cells is higher for the base cases. This is due to the additional refinements applied to the slender chamfered edges, particularly around the surfaces near the gap between the rudder and horn.

Table 5 – Generated grid details.

Simulation no.	Rudder	Number of cells	Minimum orthogonality
1	Simplified F01	$9\,925\,426$	15.40 deg
2	Base F01	$11\,430\,318$	10.82 deg
3	Simplified G01	$9\,261\,715$	15.82 deg
4	Base G01	$11\,610\,966$	14.90 deg

Fig. 5 depicts the computational grid for the base G01 on the domain mirror face (mid-positioned vertically), a cross-section of the XY-plane close to the rudder (top left) and the zoomed-in view of the surface grid near the rudder (top right). To enhance clarity related to the gap and leading edge regions, an additional image showing the volumetric mesh around the rudder is also provided (bottom). As shown in the bottom figure, the cell sizes are smaller near the gap and along the leading edge of the rudder.

2.4 Solver settings

All the computations are run in unsteady mode using a single fluid phase. Fully turbulent flow is presumed, using the $k\omega$ SST-Menter-2003 turbulence model. The reference length equals to the rudder chord, meaning $L_{ref} = 4.2$ m for F01 rudder and $L_{ref} = 6.2$ m for G01 rudder, while the reference speed is equivalent to $V_{ref} = 5$ m/s for all cases.

The boundary condition on the rudder surface is wall-function. For the base cases of the rudders, the horn also has the wall-function type patch. *Prescribed pressure - frozen pressure* is used on the domain bottom, while for the cylinder side, a far field velocity condition is used with the x-component equal to $V_x = -5$ m/s.

For the simplified F01 and G01 rudders, a solid body is defined using the surfaces of the rudder and for this body the rotational degree of freedom around the z-axis is imposed with a *classic ramp*. The settings are such that at $t = 2$ s, the rotation rate is smoothly increased from $0\,°/$s to $1\,°/$s at $t = 4$ s. The remaining degrees of freedom are treated as fixed, meaning they will not evolve during the simulation.

For the base F01 and G01 cases, two separate bodies need to be created: 1) the blade and 2) the horn. In this setup, the *horn* is assigned a rotational degree of freedom around the z-axis, following the same classical ramp profile as before. In addition, the *rudder* is configured to be rigidly connected to the horn, ensuring that in the simulations, the rudder and horn remain aligned.

The flow field across the entire domain is initialised at -5 m/s, while the turbulence quantities are kept at their default settings for both the boundary and initial conditions.

Computations are conducted in unsteady mode with a time step of $\Delta t = 0.01$ s. The number of time steps for the simulations are $38\,000$ with the uniform time-step law, which ensures that there is overlap between the beginning and end of the computations. During each time step, a maximum of eight non-linear iterations are executed. Also, the convergence criteria that specify the maximum number of orders of magnitude by which

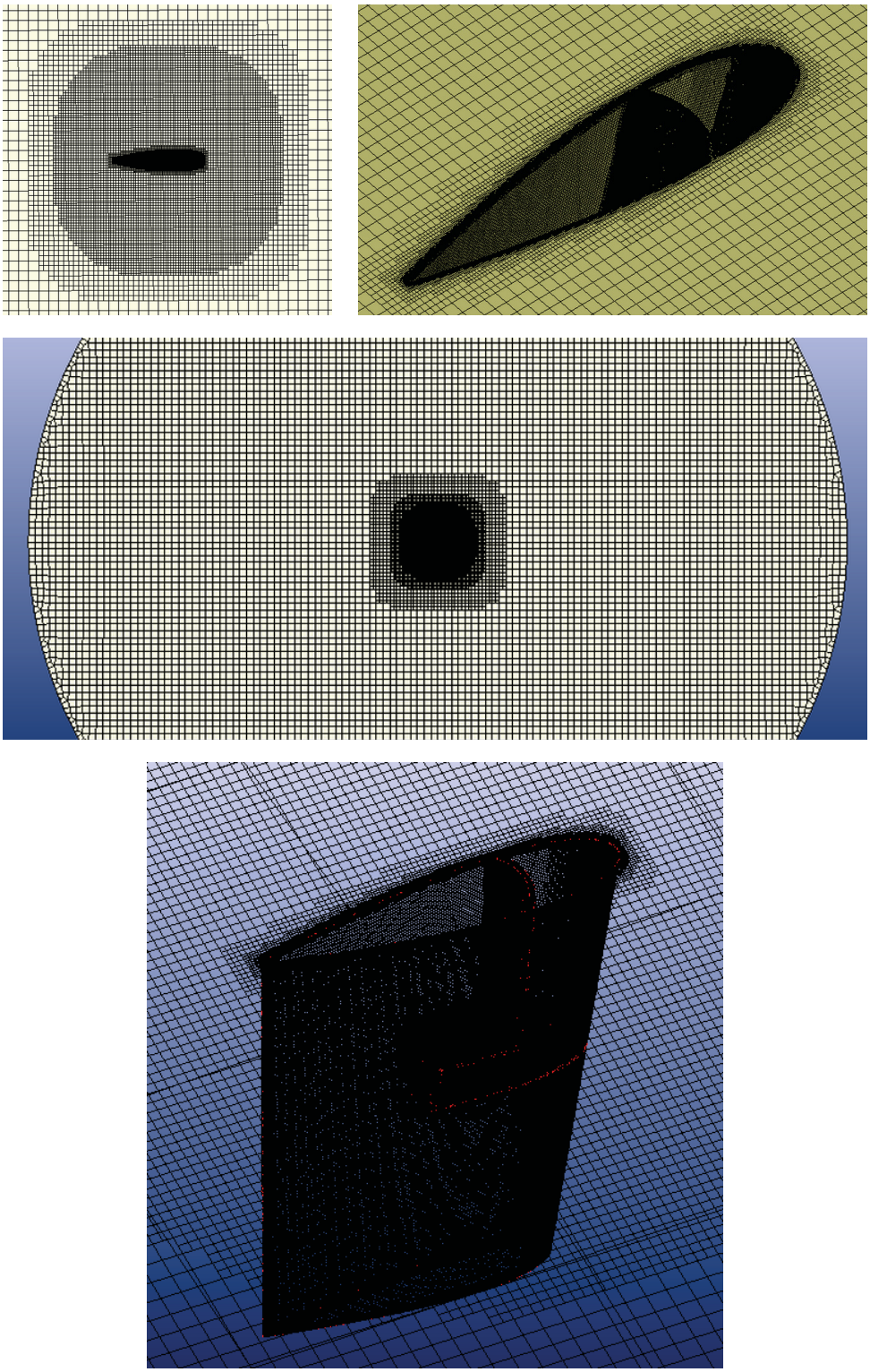

Figure 5 – Visualisations of the computational grid.

the infinite norm of the residuals must decrease during each time step is set to be 2. If this criterion is not met, the solver continues until the maximum allowed number of non-linear iterations is performed.

In Van Hoydonck *et al.* (2024), in addition to the unsteady simulations, steady simulations were performed at 12 different angles of attack to compare with the results of the averaged values of unsteady computations and reasonable agreement was observed. Consequently, to avoid duplicating previous work, this report concentrates only on unsteady simulations.

Likewise, a grid convergence study is not performed here since the setup closely follows the methodology outlined by Van Hoydonck *et al.* (2018).

3 Results and discussion

The targeted results of this study are the longitudinal (drag) force X, the lateral (lift) force Y and yawing moment N (around the Z-axis) coefficients. The coefficients are calculated in the non-dimensional format, obtained from the output of FINE/Marine as:

$$X = \frac{F_x}{\frac{1}{2}\rho V_{ref}^2 L_{ref} b}, \tag{1}$$

$$Y = \frac{F_y}{\frac{1}{2}\rho V_{ref}^2 L_{ref} b}, \tag{2}$$

$$N = \frac{M_z}{\frac{1}{2}\rho V_{ref}^2 L_{ref}^2 b}. \tag{3}$$

The raw CFD results needed additional processing to determine the mean values of the force and moment components. For each force component, the resulting curves (with increment and decrement of angle of attack) were consolidated into a single curve spanning the full range of interest. These series were then duplicated and reversed to produce the averaging process. Note that for Y and N, the values of the duplicates are negated as well. It is also important to mention that a Savitsky-Golay filter is applied to eliminate high-frequency fluctuations, particularly near the $180°$ region (for all four computations).

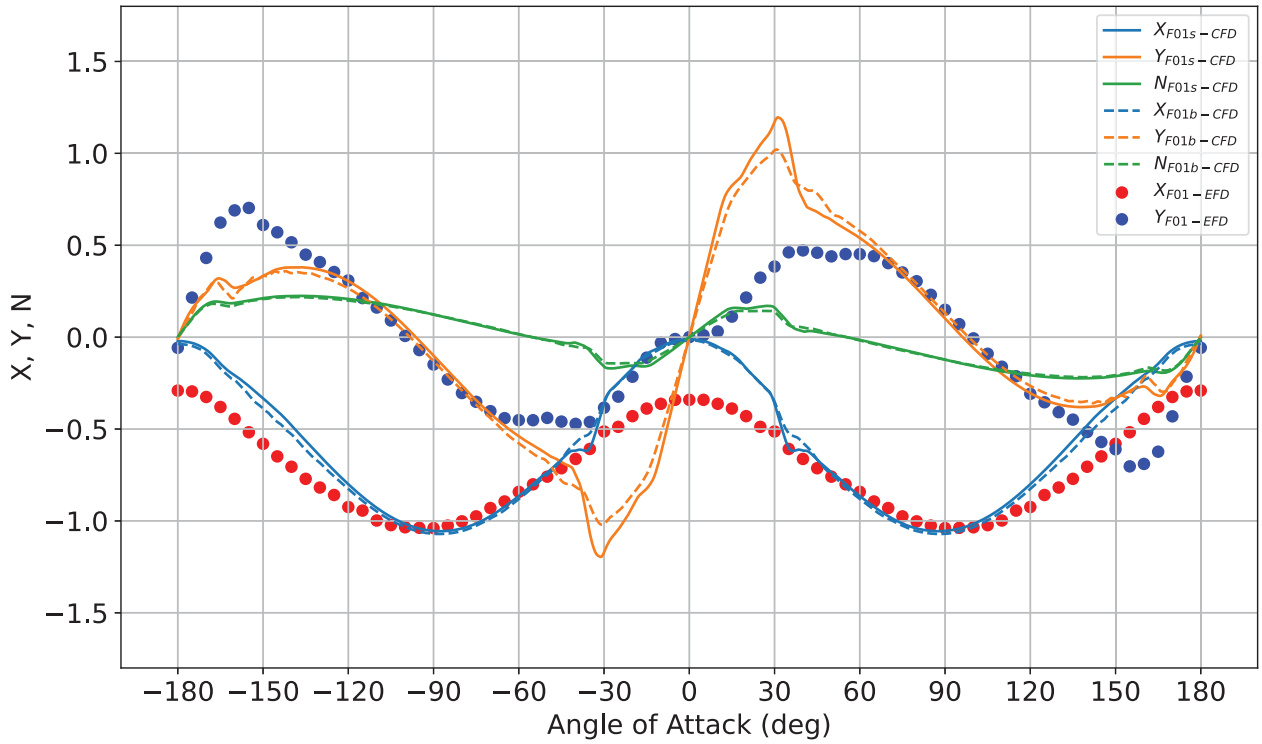

Figure 6 – Comparison of the longitudinal force (X), lateral force (Y) and yawing moment (N) coefficients of F01 rudder with experimental data.

Figure 6 shows the comparison between CFD results for the two F01 rudder configurations: the simplified F01 (denoted as *F01s*) and the base F01 (denoted as *F01b*), with the available experimental data.

One of the important things that can be easily noticed in Figure 6 is the considerable difference between the C_L calculated from CFD and the experimental data. As already pointed out in the introduction, there is at least a three order of magnitude difference with respect to the Reynolds number from what is obtained in the towing tank tests to what reality is. A key point to highlight is that in open water rudder tests, only the movable part (rudder blade) is evaluated, with the fixed portion attached to the hull not being considered. Meanwhile, the geometry of the rudder blade plus horn is simulated in CFD.

Comparison of the CFD-obtained coefficients informs us of the higher $C_{L,max}$ for the simplified rudder case. This is due to the fact that the simplified rudder maintains continuous flow over its surface; while the gap between horn and blade in the base case disturbs the flow over the rudder and enables pressure equalisation between both sides of the rudder, leading to rather early stall and reduced $C_{L,max}$. The gap also enforces flow leakage, weakening the pressure difference across the rudder.

While the base rudder generates lower peak-lift, the horn and gap increase the drag force (in some specific angle of attack ranges near stall, between $30°$ to $50°$) probably due to separation zones forming near the horn and rudder junction, plus increased pressure drag that may be caused by vortices and turbulent interactions around the gap.

Fig. 7 shows the comparison between the CFD results for G01 rudders with the existing experimental data.

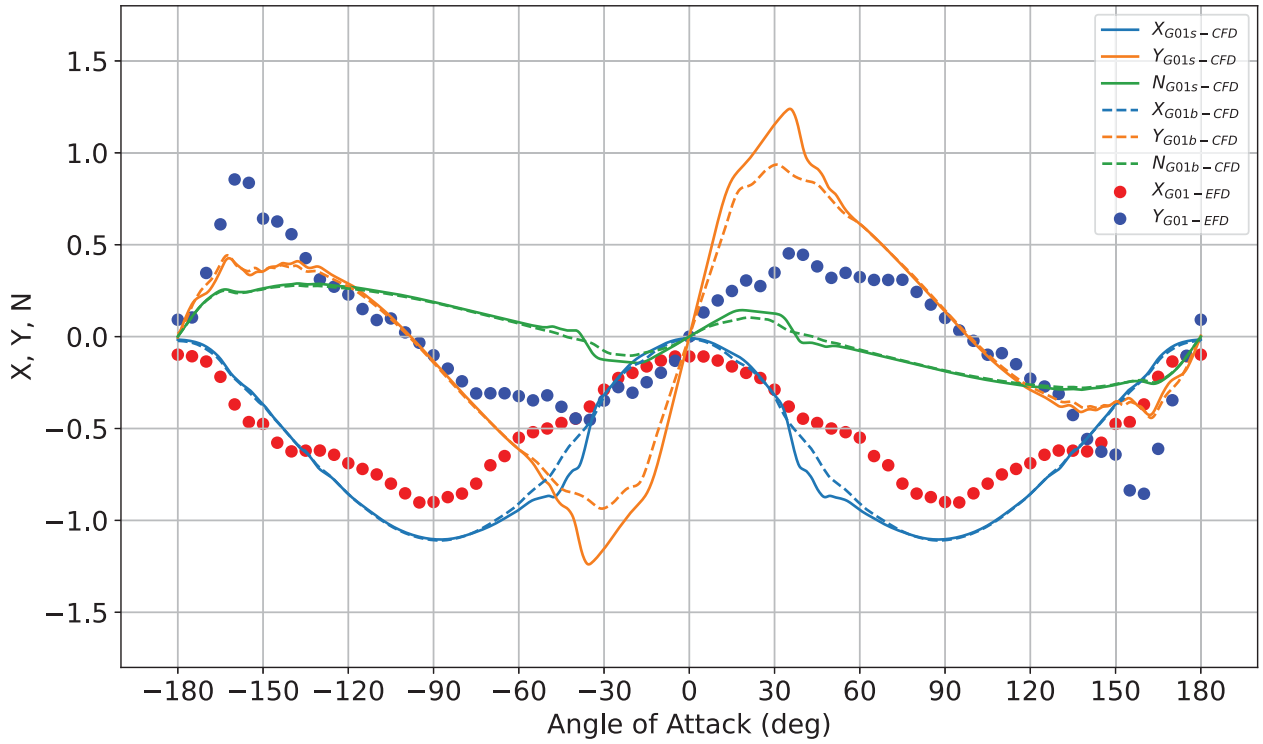

Figure 7 – Comparison of the longitudinal force (X), lateral force (Y) and yawing moment (N) coefficients of G01 rudder with experimental data.

Similar to the F01 case, the simplified G01 demonstrates a relatively higher peak lift. However, this configuration also reveals some flow instability, as evidenced by fluctuations in both lift and drag curves specifically in the reverse flow condition. Due to the single continuous surface of this rudder, the flow moves smoothly across the rudder without being interrupted by any gap.

On the other hand, the base geometry exhibits a somewhat similar trend, though some noticeable differences in drag are observed, particularly at angles of attack between $30°$ and $60°$. These variations are likely due to localised flow separation or detachment.

After comparing the CFD and experimental results, it may be beneficial to focus on the CFD-obtained results

while also considering the separate contributions of the blade and horn. Fig. 8 presents a comparison of the force and moment coefficients obtained from CFD for the base F01 rudder.

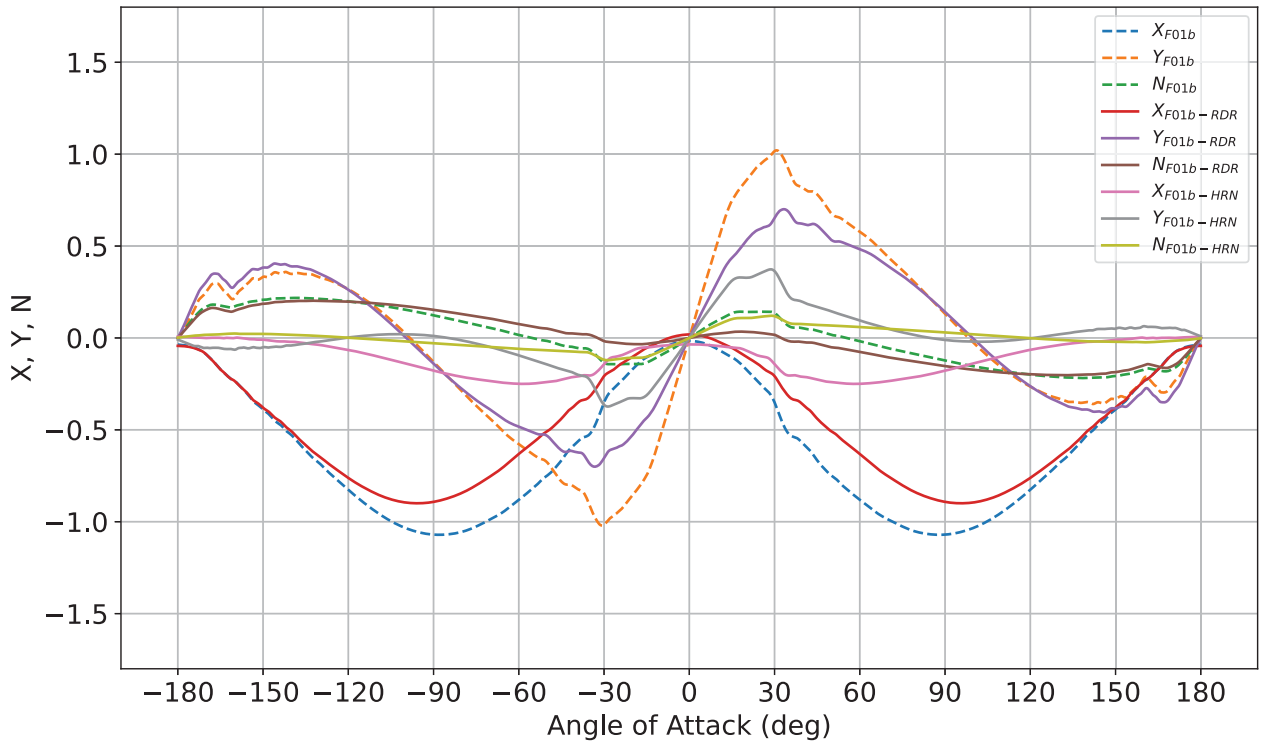

Figure 8 – Results of the longitudinal force (X), lateral force (Y) and yawing moment (N) coefficients for F01b considering the separate contribution of rudder (RDR) and horn (HRN).

As can be observed, the influence of the horn on the longitudinal force X appears to be less significant compared to the blade. A similar pattern is visible in the lift coefficient. Meanwhile, the moment coefficient seems to be dominated by the horn especially up to $40°$. This can be expected as the horn changes the pressure distribution and the resulting moments acting on the system.

Fig. 9 provides a comparison of the force and moment coefficients obtained from CFD for the base G01 rudder including the individual contributions of the blade and horn.

Overall, the results indicate a similar trend when comparing the performance of this rudder geometry to F01, in terms of the separate contributions of the horn and rudder. The drag in F01 is somewhat higher, suggesting that G01 may be more efficient due to the drag reduction. The peak lift in this rudder is lower, with smoother fluctuations compared to the F01 rudder. Also, the moment coefficient in F01 shows greater variations with more pronounced peaks and troughs.

Fig. 10 and Fig. 11 outline the comparison of X and Y force coefficients between the base F01 and G01 - considering only the contribution of the rudder blade (excluding the horn) - with the Experimental Fluid Dynamics (EFD) results. This is admittedly not a fair comparison, as the horn is present in the CFD simulations but absent in the open water rudder tests. Nevertheless, the intention is to make a general comparison while considering the differences between the cases.

As shown in Fig. 10, the CFD results underestimate the drag force. While the overall trend of the drag data mirrors the experimental results - both display a somewhat sinusoidal pattern with minimum values near $-90°$ and $90°$, the amplitude in the CFD data is indeed lower. Additionally, the lift curve slope under normal flow condition is steeper in the CFD results compared to the EFD, which is expected. Consequently, the $C_{L,max}$ is higher in CFD near $0°$. The opposite trend is observed under reverse flow condition. Moreover, there is reasonable agreement between CFD and EFD results only within a limited angle of attack range, specifically

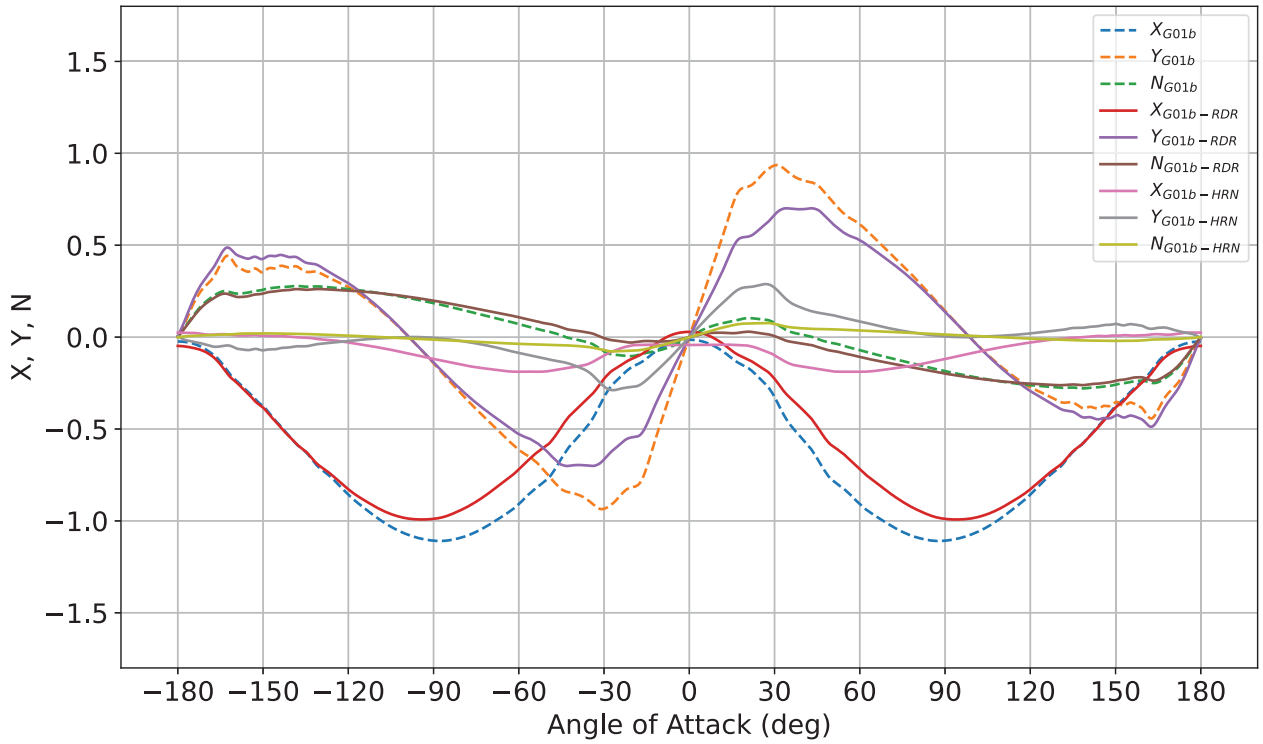

Figure 9 – Results of the longitudinal force (X), lateral force (Y) and yawing moment (N) coefficients for G01b considering the separate contribution of rudder (RDR) and horn (HRN).

from $60°$ to $120°$ and $-120°$ to $-60°$. In Fig. 11, the lift curve continues to display behavior similar to that of the base F01 rudder. However, the significant discrepancy observed in the drag curve earlier is no longer present.

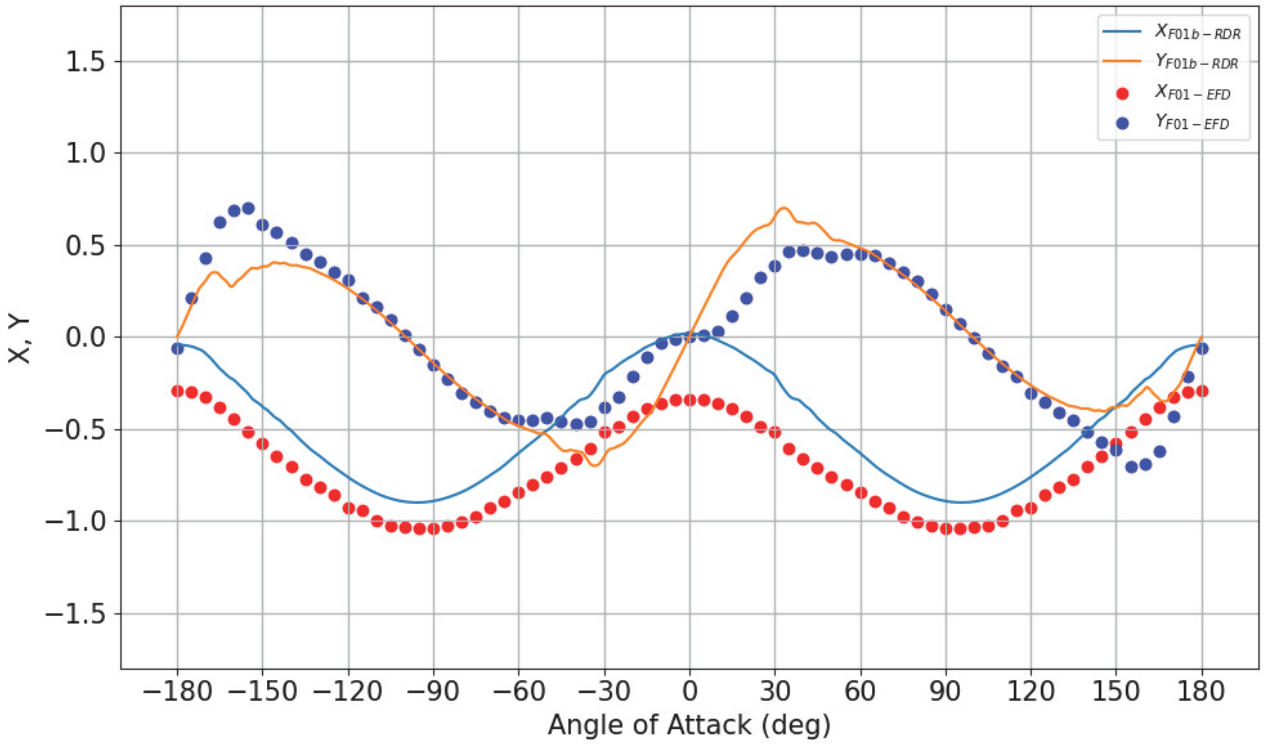

Figure 10 – Results of the longitudinal force (X) and lateral force (Y) coefficients for F01b considering only the contribution of rudder (RDR) compared with experimental data.

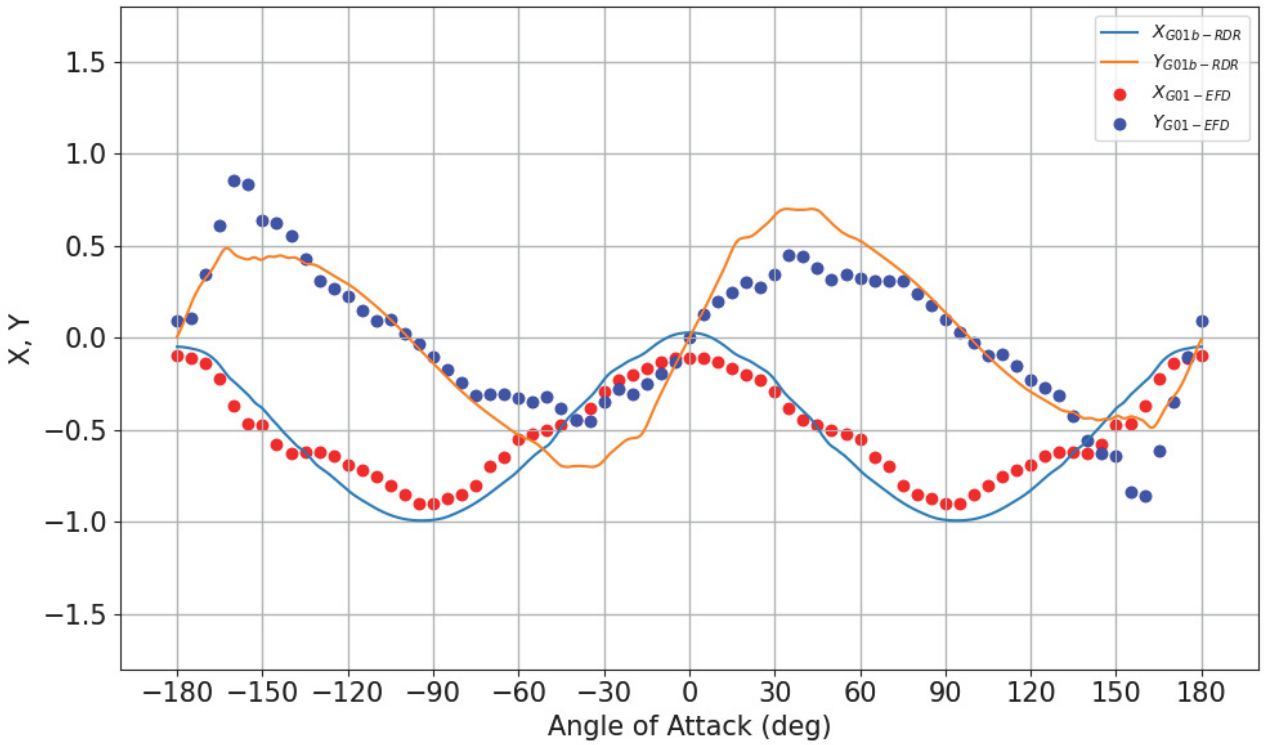

Figure 11 – Results of the longitudinal force (X) and lateral force (Y) coefficients for G01b considering only the contribution of rudder (RDR) compared with experimental data.

4 Conclusions

This report focuses on calculating the open-water rudder characteristics for the rudders of the Grand Princess (F01) and Al Shamal (G01). For comparison, two configurations are analyzed for each rudder: a simplified geometry and a base geometry. The numerical simulations, conducted using FINE/Marine, determine the drag, lift and yawing coefficients of the rudders, with a symmetry plane applied at the top side. Unsteady simulations are employed to evaluate the coefficients over the entire range of angles of attack, achieved by gradually rotating the rudder around its stock. To address hysteresis effects near stall, the final results are obtained by averaging two data sets: one with increasing angles of attack and the other with decreasing angles of attack. Owing to the lateral symmetry of the rudders, a single computation for each configuration is sufficient to cover the full range of angles of attack (from $\alpha = 0°$ to $360°$).

The CFD results are shown to be qualitatively correct over the range of angles of attack. While comparing the results with the available experimental data leads to high discrepencies especially for the lift coefficient. This is caused by the difference in Reynolds number between experimental and CFD results, and the difference in geometry tested with both methods (i.e. lack of horn in the experiments).

A generic point to note is that an analysis of available open-water rudder data sets (at FH) has shown that for the majority of rudders tested in the towing tank, the maximum lift coefficient $C_{L,max}$ in the astern flow condition is equal or higher than the maximum lift coefficient in the ahead flow condition. Furthermore, the lift curve slope $dC_L/d\alpha$ astern is higher than ahead. These results show that when data is required for the full range of angles of attack, model scale (towing tank) results may not give correct results for all angles of attack, while such qualitative errors are not present in CFD. Indeed, the best way to validate the CFD results quantitatively could be comparing them with the suitable experimental data for similar conditions as used in unsteady CFD computations (i.e. sufficiently high Reynolds numbers); however, such data are scarse in the existing literature, especially when data for the full range of angles of attack is required.

As future research mathematical models can be derived using the obtained CFD results extracted from this study. Then, the performance of these models can be compared to a mathematical manoeuvring model that utilises the experimentally obtained open-water rudder characteristics. This can provide us with better insight about the reliability and performance of the CFD-obtained model compared to the traditional experimental open-water rudder derived models.

References

Van Hoydonck, **W.; Delefortrie**, **G.; De Maerschalck**, **B.; Vantorre**, **M.** (2018). Open-Water Rudder Tests using CFD. ***in****: proceedings of the 32nd Symposium on Naval Hydrodynamics, Hamburg, Germany, 5–10 August 2018*

Van Hoydonck, **W.; Delefortrie**, **G.; De Maerschalck**, **B.; Vantorre**, **M.; Peeters**, **P.; Mostaert**, **F.** (2017). Analysis of open-water rudders tests. Version 4.0. *FHR Reports*, 00_057_5. Flanders Hydraulics Research: Antwerp

Van Hoydonck, **W.; Panahi**, **S.; López Castaño**, **S.; Eloot**, **K.** (2024). Computation of Rudder Open Water Characteristics: Charles Darwin (H40). Version 3.0. *FH Reports*, 17_025_1. Flanders Hydraulics: Antwerp

Vantorre, **M.** (2002a). Roerkrachten in open water: deel 1. Tekst. *WL Rapporten*, 602. Waterbouwkundig Laboratorium/Universiteit Gent: Antwerpen. VI, 20 pp.

Vantorre, **M.** (2002b). Roerkrachten in open water: deel 2. Figuren, tabellen en bijlagen. Version 3.0. *WL Rapporten*, 602. Waterbouwkundig Laboratorium/Universiteit Gent: Antwerpen. VI + 12 p. figures, 3 p. tables, 106 p. appendices pp.

Vantorre, **M.** (2001). Stationary and non-stationary open water rudder tests. ***in****:* Kijima, K. (Ed.). *Mini Symposium on Prediction of Ship Manoeuvring Performance, 18 October 2001, Tokyo, Japan.* Japan Marine Dynamics Research Sub-Committee. 103–111 pp.

A1 Coefficient values

The numerical values of the longitudinal force (X), lateral force (Y) and yawing moment (N) coefficients for the F01 (simplified and base) and G01 (simplified and base) rudders are provided in the lists below.

Listing A1.1 – Coefficient values of F01s.

```
# density: 999.1026 kg/m^3
# Lref: 4.2 m
# draft: 7 m
# Vref: 5 m/s
# Fndim: 0.5 * density * Vref^2 * Lref * draft
# Mndim: 0.5 * density * Vref^2 * Lref^2 * draft
AoA,X,Y,N
-180.0,-0.02053914179695874,-0.00808949049932818,0.0006522375947070175
-175.0,-0.03145855663437427,0.15429089251121236,0.10361632296307842
-170.0,-0.06898009415040375,0.24132082584449605,0.17767580583417067
-165.0,-0.1445963349252089,0.318186080416712,0.19164841421731804
-160.0,-0.20680654879908458,0.26848368112070803,0.18601663330927573
-155.0,-0.2660110618476884,0.2924933479537259,0.20049221543436394
-150.0,-0.33289170438220245,0.33290147966061717,0.2122809921647744
-145.0,-0.40153757584378363,0.3696038674101247,0.22096016661149062
-140.0,-0.4798411769688712,0.3795770037310252,0.2238450250321774
-135.0,-0.5638682751139207,0.3786314428754544,0.224238001291298
-130.0,-0.646270194742976,0.3664441689804037,0.2213753946976581
-125.0,-0.7257280256934736,0.3418130715437653,0.2158002200238349
-120.0,-0.8002220469069972,0.3048760738459 1975,0.20789686330546847
-115.0,-0.8684570487781382,0.2572000777541637,0.198018779781676
-110.0,-0.9285168735612361,0.19972680424488576,0.1861512199184344
-105.0,-0.9781783705972418,0.1333681882551686,0.17248820635404563
-100.0,-1.0160198874851774,0.059674801282002296,0.1572546619216156
-95.0,-1.0414910505977313,-0.01912033631265899,0.140683975667297
-90.0,-1.0544671452350014,-0.10096158877501438,0.12310147946829236
-85.0,-1.054055154758476,-0.18377592818089328,0.1048661552088915
-80.0,-1.0408007590996033,-0.2653746655405595,0.08636011070749448
-75.0,-1.0140434102390274,-0.34359157449939814,0.06789752922029854
-70.0,-0.9739405545028541,-0.4164976868110397,0.04988646617886336
-65.0,-0.9227693133590595,-0.48205375989402427,0.03227536908484138
-60.0,-0.864847621506066,-0.5394386798582886,0.014957105031630136
-55.0,-0.7993780823864957,-0.5882435924996985,-0.0011714059961228053
-50.0,-0.7359810658583669,-0.6377571546476863,-0.01502967911001564
-45.0,-0.6671948796039512,-0.6810391222944986,-0.028373337945450293
-40.0,-0.6173384730123233,-0.749775929689534,-0.030347497204375993
-35.0,-0.6024109796482536,-1.0676216882768808,-0.07454214963952666
-30.0,-0.3614019367199357,-1.170907647257534,-0.16103011075229343
-25.0,-0.24875763185397146,-1.047191621179332,-0.16641860794676322
-20.0,-0.16980562410355332,-0.9231493457336266,-0.15455166780800622
-15.0,-0.09183644171188597,-0.8244016292001322,-0.15787945722305038
-10.0,-0.051651143391647523,-0.632926665813073,-0.11477351097959254
```

```
-5.0,-0.020806240592815446,-0.31342892708837355,-0.05877863407793929
0.0,-0.010729569569023979,1.4271435753632942e-06,2.707471420837362e-07
5.0,-0.020806443321878598,0.31343228892037434,0.05877925221790508
10.0,-0.051651551243002226,0.6329296926092177,0.11477402428676213
15.0,-0.09183693586925494,0.8244024875950516,0.15787963161206717
20.0,-0.16980653581591473,0.9231508886756097,0.15455171411325408
25.0,-0.24875836203413407,1.04719263486344,0.1664187427307107
30.0,-0.3614044622510564,1.1709095629528887,0.16102950730101898
35.0,-0.602412153019269,1.0676181141823444,0.07454131968383668
40.0,-0.6173385700351124,0.7497739802650417,0.03034725563106842
45.0,-0.6671956895835008,0.6810386303875533,0.02837317394531851
50.0,-0.735981575405911,0.6377566223207582,0.015029566639042268
55.0,-0.7993787807776134,0.5882431356382036,0.0011712494541233505
60.0,-0.8648482422676541,0.5394381228636012,-0.014957278592824086
65.0,-0.9227698136593755,0.4820532085096215,-0.03227552694076598
70.0,-0.9739410765111477,0.41649690008283086,-0.04988666758874271
75.0,-1.0140437130830455,0.34359087644511194,-0.06789769647852506
80.0,-1.0408009635386757,0.26537388879391693,-0.08636029054835594
85.0,-1.054055216394422,0.18377505343007047,-0.10486635077065136
90.0,-1.054467085725345,0.10096082877755017,-0.12310164389781705
95.0,-1.0414908454196206,0.019119447992342133,-0.14068416443801385
100.0,-1.0160195782609918,-0.05967553124294423,-0.15725481364283947
105.0,-0.9781779529206402,-0.1333688704294741,-0.17248834721445033
110.0,-0.9285162591112256,-0.1997274853137714,-0.1861513599020033
115.0,-0.8684564443934981,-0.2572005711650081,-0.19801888166348652
120.0,-0.8002213101380472,-0.304876520629444,-0.20789695648512652
125.0,-0.7257272515757553,-0.3418133738624704,-0.215800286711663
130.0,-0.646269455331736,-0.36644433779234503,-0.22137543432141363
135.0,-0.5638673405267308,-0.378631521123655,-0.22423801771569443
140.0,-0.4798403886828382,-0.37957696783025713,-0.22384500365733725
145.0,-0.4015368736213303,-0.36960367425757423,-0.22096012112369154
150.0,-0.3328910189448422,-0.33290110089038527,-0.21228088776950335
155.0,-0.26601046163318803,-0.29249281181529746,-0.20049207174886627
160.0,-0.2068059520433421,-0.26848373599185776,-0.1860165056826603
165.0,-0.14459561855169709,-0.3181861053570529,-0.1916484980427213
170.0,-0.06897953269496532,-0.24131988560971301,-0.17767537271324355
175.0,-0.03145832514952403,-0.15429044740174863,-0.10361866891000557
180.0,-0.020539363160427773,0.008098948093512942,-0.0006160436987525386
```

Listing A1.2 – Coefficient values of F01b.

```
# density: 999.1026 kg/m^3
# Lref: 4.2 m
# draft: 7 m
# Vref: 5 m/s
# Fndim: 0.5 * density * Vref^2 * Lref * draft
# Mndim: 0.5 * density * Vref^2 * Lref^2 * draft
AoA,X_combined,Y_combined,N_combined
-180.0,-0.0359459060093806,-0.007796897560922021,0.0017040564796037096
-175.0,-0.04791056035191851,0.131491095013015,0.09954812150821446
-170.0,-0.0897153337613675,0.25179557274331793,0.16978581332276588
-165.0,-0.17168167380573202,0.2789791928020223,0.17576736137980822
-160.0,-0.23340474938516945,0.21906831984593036,0.17208434620474133
-155.0,-0.31588545116669353,0.3022870017073917,0.19569941145438566
-150.0,-0.38920312101045584,0.3323213543520063,0.2079076819358676
-145.0,-0.46098711302744855,0.35468254436384683,0.2149734886726121
-140.0,-0.5284566263585297,0.34832932977878,0.21716570733427096
-135.0,-0.6119014905947594,0.34741303165979076,0.21593452830953602
-130.0,-0.6840202565106454,0.3288824001955299,0.21291354839868415
-125.0,-0.7577858488971405,0.30317993175231994,0.20714253273766312
-120.0,-0.8260621858547401,0.26501617103310854,0.1992534425182627
-115.0,-0.8908696889651849,0.21802699722297406,0.1902375231670484
-110.0,-0.9485032828195562,0.16213354049501078,0.17951933799708636
-105.0,-0.996779899322624,0.09759129280694062,0.16754647174753023
-100.0,-1.0336129576780013,0.025947021377035525,0.15412904443298905
-95.0,-1.0580447407833276,-0.050904176170301366,0.13922516689979106
-90.0,-1.070011145409295,-0.13081150831939775,0.12321807723831543
-85.0,-1.0686671913036643,-0.21157324501601135,0.10655134366654838
-80.0,-1.054947721065716,-0.29146907730049587,0.08954177179214472
-75.0,-1.025977018472848,-0.3687105973304692,0.0728317085229628
-70.0,-0.9879715269718727,-0.4396294779217398,0.055946984102486136
-65.0,-0.9413815200256401,-0.5168563023061754,0.03592662058434172
-60.0,-0.8806053406917796,-0.5775329774693977,0.016330080656659134
-55.0,-0.817586957982537,-0.6335686198004998,-0.0015021714752987663
-50.0,-0.7487668888421508,-0.6773193589493443,-0.01638881861773461
-45.0,-0.6660040236431537,-0.7811330865912129,-0.03955491897161223
-40.0,-0.5744009973719401,-0.8157695819287618,-0.05243456054039496
-35.0,-0.5225774613420396,-0.9142942443270629,-0.06463662877041151
-30.0,-0.35032172705632547,-1.0163959726562994,-0.13597529590528165
-25.0,-0.2508007200424879,-0.9454199218690554,-0.14321350912865188
-20.0,-0.17066471573958278,-0.8561587601392038,-0.14159200672243857
-15.0,-0.10527246434899358,-0.7465329689651413,-0.13465024016333854
-10.0,-0.061267430171145304,-0.5244000193649991,-0.09510898782503387
-5.0,-0.02770505391195432,-0.2688507410758596,-0.050694959071243974
0.0,-0.016048596751601092,1.2972984161428682e-06,2.360861453094476e-07
5.0,-0.027705314494315743,0.26885344882065854,0.05069550092995168
10.0,-0.061267858970015396,0.5244024044687009,0.0951093870724493
15.0,-0.10527278717533893,0.7465343623779543,0.13465058608409378
20.0,-0.17066555128323221,0.8561597608273407,0.1415919820446516
25.0,-0.2508015034856993,0.9454206800591664,0.14321346652973288
30.0,-0.3503236575276816,1.0163967066276673,0.13597483655861828
```

```
35.0,−0.5225781919003479,0.914292408350362,0.06463624061529266
40.0,−0.574401878871215,0.8157690829117449,0.05243434878644736
45.0,−0.6660052316782964,0.7811324016058436,0.03955468430563028
50.0,−0.7487674337358325,0.6773185100021033,0.016388636264604624
55.0,−0.8175877794808635,0.6335682114275173,0.0015020076940709059
60.0,−0.8806060385068191,0.577532505296442 8,−0.016330260332398136
65.0,−0.941381980405882,0.516855617275344,−0.0359268132555041
70.0,−0.9879719562079176,0.4396286368472538,−0.05594718873035956
75.0,−1.0259772099792903,0.36870989205499277,−0.0728318580069506
80.0,−1.054947955681135,0.2914683096360879,−0.08954193557921693
85.0,−1.0686672356425229,0.2115723867937132,−0.10655152177646114
90.0,−1.0700111972873847,0.13081076510643164,−0.12321822881688996
95.0,−1.0580445250174988,0.05090331128440127,−0.13922533748021984
100.0,−1.033612732181874,−0.025947739559616968,−0.1541291783306108
105.0,−0.9967795282116496,−0.09759198283261285,−0.16754659831051927
110.0,−0.9485027803861588,−0.16213424319739791,−0.17951946400514918
115.0,−0.8908692080772576,−0.21802751826463324,−0.1902376186337922
120.0,−0.8260616018138267,−0.26501666644140426,−0.19925353683297378
125.0,−0.757785150149413 5,−0.30318023558731766,−0.2071425849053457
130.0,−0.6840195112760629,−0.32888250943377273,−0.2129135782709328
135.0,−0.6119005416031918,−0.3474130095662985,−0.21593453913110297
140.0,−0.5284559480657328,−0.348329215845364,−0.21716565239348573
145.0,−0.4609865481113296,−0.35468282996782985,−0.2149735053758035
150.0,−0.3892024162460009,−0.3323211030526849,−0.20790763941106072
155.0,−0.3158845349167416,−0.30228582582906793,−0.19569918433743197
160.0,−0.2334041972857276,−0.219067478616139,−0.17208400329631293
165.0,−0.1716809715916951,−0.2789803505185981,−0.17576748130459066
170.0,−0.08971459992936004,−0.2517943329215445,−0.16978550743783902
175.0,−0.04791040950749011,−0.13147765503941955,−0.09955269026988395
180.0,−0.03594514090985071,0.007673125645962675,−0.0016451600260385668
```

Listing A1.3 – Coefficient values of G01s.

```
# density: 999.1026 kg/m^3
# Lref: 6.2 m
# draft: 10.4 m
# Vref: 5 m/s
# Fndim: 0.5 * density * Vref^2 * Lref * draft
# Mndim: 0.5 * density * Vref^2 * Lref^2 * draft
AoA,X,Y,N
-180.0,-0.01607459422529826,-0.004449151098963191,0.0003777284417324083
-175.0,-0.025320088723904722,0.1772136183259082,0.10903042762740571
-170.0,-0.05439157037519367,0.2353372099544322,0.19733977871327968
-165.0,-0.12055248103585495,0.3590349750044813,0.25089751701103763
-160.0,-0.22235331526586627,0.4034489845248455,0.24529466882868306
-155.0,-0.2870411295314347,0.3360645397031818,0.24404904730853144
-150.0,-0.3683591894099709,0.3548151310287545,0.26231747338984496
-145.0,-0.460941084838672,0.38443732192010127,0.27685784390858487
-140.0,-0.5518062455892069,0.39756388893907596,0.2845665313234311
-135.0,-0.6290948232699493,0.38158693953215,0.2848205561561858
-130.0,-0.7222774313003923,0.378286856106964,0.28710027468927124
-125.0,-0.7786186734442919,0.3291096584894007,0.27725125024657854
-120.0,-0.8566876192527666,0.29002414877689464,0.27148206024070415
-115.0,-0.9198766307668147,0.23783879682251238,0.26143230316766436
-110.0,-0.9768237829292816,0.17640768457547493,0.24919647719996407
-105.0,-1.0272065559216035,0.10757543332016849,0.2366119373017879
-100.0,-1.06451894120605,0.031055959487196284,0.22206143049512825
-95.0,-1.0894148627466957,-0.04961451065699786,0.20580579314190792
-90.0,-1.102481596704055,-0.1343156141629589,0.18852518568252047
-85.0,-1.102265768004001,-0.2202867732974503,0.17040406834855978
-80.0,-1.0878642466657498,-0.30401698641310976,0.15174364016183967
-75.0,-1.0627662029594298,-0.38569590657147135,0.133071404086988
-70.0,-1.0310346469994494,-0.4666435052235228,0.11468222888096768
-65.0,-0.989284461587374,-0.5442541390227775,0.09547534533111597
-60.0,-0.9427334288920898,-0.6134051381690924,0.07836329903075658
-55.0,-0.8894457872236836,-0.6897043419173837,0.060132071074698375
-50.0,-0.8676299522891806,-0.7945922839273697,0.050976680290577996
-45.0,-0.8276941630860808,-0.9148239945830391,0.04091016618356456
-40.0,-0.7215303445542904,-1.027774580695749,0.0340971782725005
-35.0,-0.49379599883885394,-1.2378831541799353,-0.06868393384030269
-30.0,-0.31837283674108613,-1.1545665207655897,-0.1259397720480661
-25.0,-0.22107864878846392,-1.046480823191714,-0.1339992217437965
-20.0,-0.13898216148957013,-0.9471532530618603,-0.14278043302812718
-15.0,-0.08831840258841835,-0.8537762389416976,-0.13196897927319126
-10.0,-0.048426332036480065,-0.6246937466930521,-0.09006872251082264
-5.0,-0.018834964275261986,-0.3127046882246923,-0.04636365658621608
0.0,-0.009051263741577886,1.4274053510705402e-06,2.1376369416839826e-07
5.0,-0.018835161024877048,0.3127080293123507 5,0.04636414261163485
10.0,-0.048426714433459354,0.6246965977061754,0.0900691214680957
15.0,-0.08831876504542359,0.8537776059298189,0.13196931980627846
20.0,-0.1389828709499605,0.9471541379211624,0.1427803428216433
25.0,-0.22107951402786857,1.046481782505091,0.13399915596594225
30.0,-0.31837384705812394,1.1545675675910498,0.12593963943219857
```

```
35.0,−0.4937993291899933,1.237883505073144,0.06868270082296785
40.0,−0.7215306586407453,1.027771358960522,−0.03409732443974163
45.0,−0.8276955026705326,0.9148231347453216,−0.04091037470061581
50.0,−0.8676301423716773,0.7945916913722526,−0.05097658877752796
55.0,−0.8894460939820428,0.6897032843518845,−0.06013221318528974
60.0,−0.9427339894941335,0.6134044887448046,−0.07836347770691535
65.0,−0.9892848658400639,0.5442534798103278,−0.0954755105030737
70.0,−1.031035066421111,0.4666426027300867,−0.11468244086616307
75.0,−1.062766457807965,0.3856951591329672,−0.1330715755146991
80.0,−1.087864581966888,0.3040161885365442,−0.1517438210435588
85.0,−1.102265832424533,0.22028587002527966,−0.17040426272021925
90.0,−1.1024815376975285,0.13431482317612312,−0.18852534881084193
95.0,−1.0894146580286097,0.04961359648160174,−0.20580597845611884
100.0,−1.0645186403822875,−0.031056709479700205,−0.2220615778600429
105.0,−1.0272061391873852,−0.10757614708787036,−0.23661206852974395
110.0,−0.9768231688197306,−0.17640838857758573,−0.24919660996875154
115.0,−0.9198760916592806,−0.23783935557118527,−0.2614324187817639
120.0,−0.8566868887016121,−0.29002459148546716,−0.2714821309071623
125.0,−0.7786179514685736,−0.3291100833230504,−0.2772513329855616
130.0,−0.7222768430777031,−0.3782871698387552,−0.28710031955949683
135.0,−0.6290940825050559,−0.38158750005887443,−0.284820625297456
140.0,−0.5518054947490525,−0.39756383256776745,−0.28456641804888283
145.0,−0.46094018636095563,−0.384436979797711,−0.2768577378997565
150.0,−0.36835832797279877,−0.35481478677441947,−0.2623173167960313
155.0,−0.28704068222116713,−0.3360648189563423,−0.2440488756235572
160.0,−0.22235247951607162,−0.4034499632161189,−0.24529484331393317
165.0,−0.12055162025854152,−0.3590333363045842,−0.2508971919579397
170.0,−0.05439110179534596,−0.23533656814059706,−0.19733912982424126
175.0,−0.025319922260125978,−0.1772172365830828,−0.10903235440954191
180.0,−0.016074651928441652,0.004502534105643718 5,−0.00034503842711527954
```

Listing A1.4 – Coefficient values of G01b.

```
# density: 999.1026 kg/m^3
# Lref: 6.2 m
# draft: 10.4 m
# Vref: 5 m/s
# Fndim: 0.5 * density * Vref^2 * Lref * draft
# Mndim: 0.5 * density * Vref^2 * Lref^2 * draft
AoA,X_combined,Y_combined,N_combined
-180.0,-0.02320179855934079,0.014507258763098885,0.0002913618601047339
-175.0,-0.03326973501762205,0.1667046841548562,0.10795792867887403
-170.0,-0.06830389949560504,0.2827393435615955,0.1947665791401547
-165.0,-0.13277043260554508,0.39569137699937706,0.24517035604748896
-160.0,-0.22845140689104682,0.3990972017218328,0.23775540984546314
-155.0,-0.30131284524748175,0.3563999751847484,0.24371216915378302
-150.0,-0.374414142231136,0.35426720743066326,0.2576651515709622
-145.0,-0.4634543443169136,0.37906964291354583,0.2705223885920199
-140.0,-0.5518478126993476,0.38159768319021714,0.2769826022306228
-135.0,-0.6242609592276982,0.3558469352168351,0.2743538709724146
-130.0,-0.7136729193478408,0.3491241702442521,0.2754271434182771
-125.0,-0.7782679962286027,0.3096874469710771,0.2684446137256587
-120.0,-0.8568887409885543,0.27315977212072384,0.26145304084003795
-115.0,-0.9229296435758418,0.2229619863230368,0.25300906577013343
-110.0,-0.9816376959670392,0.16383905054860834,0.241966253126146
-105.0,-1.0316255370329364,0.0961989779358388,0.22993590804186634
-100.0,-1.0692846515396623,0.021084665779768835,0.21647292335421875
-95.0,-1.0944347553507583,-0.05849704259210425,0.2013763908004159
-90.0,-1.1075744421221436,-0.14176970029630553,0.18519893751474925
-85.0,-1.1065375211096655,-0.22746910450243896,0.16755350067929495
-80.0,-1.0895932245663706,-0.3121864390767969,0.14870195808762854
-75.0,-1.0594645637443498,-0.39214784619183796,0.12983831640085028
-70.0,-1.0166975085152576,-0.46689794903988896,0.11114907948786026
-65.0,-0.9679299781583915,-0.5423424790491893,0.09176272832845091
-60.0,-0.9081982818148474,-0.6136791499688031,0.0708936203842598
-55.0,-0.8335811534219857,-0.6657856275465889,0.05034645169636409
-50.0,-0.7738374983700381,-0.7437576928124353,0.031704721564934195
-45.0,-0.659603696277467,-0.8279200898530101,0.009178533367664974
-40.0,-0.5578693541293153,-0.8526944379616116,-0.012506762241658656
-35.0,-0.46598093180477873,-0.8949697174188627,-0.031528863764887706
-30.0,-0.3256946908431192,-0.9342010768999724,-0.0776104652080829
-25.0,-0.22764779159858978,-0.874421761680883,-0.09738131798690053
-20.0,-0.16120781590691186,-0.8163170221258433,-0.1029062720269686
-15.0,-0.11636854181273813,-0.7098249115955519,-0.08491460320171135
-10.0,-0.05950067618191797,-0.4653251064495794,-0.06936231463445323
-5.0,-0.024942253587760862,-0.23174986172470677,-0.04199886285239014
0.0,-0.01413190161481165,1.0581373408021025e-06,2.1655469980488437e-07
5.0,-0.024942472215147497,0.23175223022115812,0.04199927523708272
10.0,-0.059501102587470635,0.4653272424169974,0.06936251796175345
15.0,-0.11636910607659441,0.7098270984877645,0.0849147700855905
20.0,-0.16120830678423817,0.8163171837336152,0.10290634074772037
25.0,-0.22764852131725408,0.8744226760197029,0.09738124958868959
30.0,-0.32569620655631976,0.9342013364849593,0.0776099969553342
```

```
35.0,−0.46598184460302994,0.8949690064984477,0.03152864127907451
40.0,−0.557870267087846,0.8526941632869501,0.012506584066661889
45.0,−0.6596051757185333,0.8279196362178175,−0.009178875967399327
50.0,−0.7738381020955538,0.7437568194777152,−0.0317048563866712
55.0,−0.8335818843730458,0.6657849651337834,−0.05034667107004015
60.0,−0.9081989902430603,0.6136785468173939,−0.07089383088735418
65.0,−0.9679304607337995,0.5423417753613192,−0.09176291300918635
70.0,−1.016698054160319,0.4668971180085831,−0.1111492920693942
75.0,−1.05946487056499,0.39214713740733564,−0.12983848711933413
80.0,−1.0895934533145917,0.312185639061084,−0.1487021411406273
85.0,−1.1065376422044222,0.2274681903778297,−0.16755369716276713
90.0,−1.1075743789097834,0.14176891713347556,−0.18519909404884577
95.0,−1.0944345215829927,0.05849615660396555,−0.20137656015940272
100.0,−1.0692843190452264,−0.021085398315559837,−0.21647305088840288
105.0,−1.0316251456133403,−0.09619967811121011,−0.22993603439672586
110.0,−0.9816370793102841,−0.163839741961431,−0.24196637819412609
115.0,−0.9229290753809489,−0.22296251775972975,−0.2530091625768812
120.0,−0.8568879649444983,−0.27316018131409464,−0.2614531120846113
125.0,−0.7782672181837608,−0.30968779201269225,−0.2684446857633143
130.0,−0.7136723243973333,−0.349124502861504,−0.2754271878586754
135.0,−0.6242601224259398,−0.3558472089335677,−0.27435389173689767
140.0,−0.5518470386441192,−0.381597426823298,−0.2769824653182245
145.0,−0.46345349496110133,−0.3790693884313087,−0.270522327723473
150.0,−0.37441342301134417,−0.35426701394307075,−0.25766496927535626
155.0,−0.3013122951822936,−0.3563998100344733,−0.24371193677293934
160.0,−0.22845066536770203,−0.39909853816693897,−0.2377555462335518
165.0,−0.13276962777128262,−0.3956901897357411,−0.24517002841671293
170.0,−0.06830341210196668,−0.2827385228437108,−0.1947659708725907
175.0,−0.033269557256326326,−0.16670927017198023,−0.10795951567993746
180.0,−0.02320147944994188,−0.014439007577556562,−0.00026233441508141664
```

A2 Access guide for experimental data

This appendix provides guidance on locating experimental data for open-water rudder characteristics (including C_D and C_L) to facilitate comparison between numerical results and existing experiments. Considering the volume/variability of available data, this manual aims to offer a clear method for users to efficiently find the information they require.

Indeed, wlsow.vlaanderen.be website contains a significant amount of experimental data. Specifically, by navigating to the ”Scheepsdatabank”, one can access various details related to the experimental database of ships. On the left side of the webpage, there is a list of all available ship hulls (”Lijsten” -> ”Scheepsrompen”). This section provides information on all the ships included in the database. Given that this report focuses on the F01 and G01 rudders, we can simply search for their names and investigate the following:

- **F01** corresponds to the Grand Princess ferry ship;
- **G01** corresponds to the Al Shamal gastanker.

Once we’ve identified which ships the rudders belong to, we can search for the section that provides more details about the rudder itself. By opening the ”Projecten” section, we will find various project site URLs. From there, we need to access ”Roeren”. Under ”Bibliotheken”, there are several tabs like ”Autopilotbestanden”, ”Trajectbestanden”, ”Excelbestanden”, etc. Our focus should be on ”Excelbestanden”, which contains a list of Excel files, and sometimes zip files that also contain Excel files. It’s crucial to know that the files ”R1F01” and ”R1G01” correspond to the F01 and G01 rudders, respectively. When we open these files, we’ll find a sheet labeled ”geselecteerd” at the bottom, which contains the final C_D and C_L values used as inputs for simulators as well.

The explanation above refers to tracking various types of data we need as a general guide, in addition to details on locating experimental open water data for rudders. There is also a quicker method to obtain open water rudder characteristics. By accessing ”Scheepsdatabank” and selecting ”Openwaterkarakteristieken” from the left-side menu, you can instantly retrieve the available open water data.

To better understand the structure, naming/labeling process of the rudders, it is highly recommended to review (Vantorre, 2002a) and (Vantorre, 2002b).

DEPARTMENT **MOBILITY & PUBLIC WORKS**
Flanders Hydraulics

Berchemlei 115, 2140 Antwerp
T +32 (0)3 224 60 35
F +32 (0)3 224 60 36
waterbouwkundiglabo@vlaanderen.be
www.flandershydraulics.be